

Chapter 2

Liquid-Phase Pulsed Laser Ablation

§ 2.1 Introduction

Pulsed laser ablation (PLA) was first developed in the 1960s, shortly after the invention of the pulsed ruby laser. Since then, laser ablation in a vacuum or dilute gas has been studied by many researchers. By using different target materials and background gases, and varying parameters such as the laser wavelength, fluence, and pulse duration, it is possible to produce a wide variety of thin films. These include high temperature superconductors [1], metals, semiconductors, oxides, and other ceramics [2], and diamond-like carbon [3]. The thin films have a variety of applications, for example semiconductor devices, electrodes, and wear-resistant coatings [4].

The introduction of pulsed laser ablation at the solid-liquid interface was first reported by Patil and co-workers in 1987, who used a pulsed laser to ablate a pure iron target in water to form iron oxides with metastable phases [5]. This method is known as Liquid Phase Pulsed Laser Ablation (LP-PLA), in which a solid target is immersed in a liquid medium and the laser beam is focused through the liquid onto the target surface. Following their work, Ogale [6] extended the potential of LP-PLA for the surface modification of metals, such as metallic oxidation, nitriding, and carbiding. This pioneering work opened new routes for materials processing based on the PLA of solids in various liquids. Since then, the LP-PLA method has been used to produce a wide range of novel materials, such as nanodiamond and related nanocrystals, metallic nanocrystals, nanocrystal alloys, and metal oxides. A summary of the nanocrystals synthesized by LP-PLA is listed in Table 1.

Table 2.1 Nanomaterials synthesis via LP-PLA in various liquids. (NP = nanoparticles, NR = nanrods, SDS=sodium dodecyl sulfate, LDA=lauryl dimethylaminoacetic acid, CTBA=cetyltrimethylammonium bromide)

Product	Solid Target	Liquid Solution	Laser parameters
Ag NP	Ag	H ₂ O [7, 8] C ₂ H ₅ OH [9]	Nd: YAG laser (355, 532, 1064 nm) Laser energy: 90-340 mJ/pulse Cu vapour laser (510.5 nm) Laser fluence: 1-20 J/cm ²
Au NP	Au	H ₂ O [10] Alkane liquid [11]	Nd: YAG laser (532, 266 nm) Laser fluence: 5-250 J/cm ² Nd: YAG laser (532 nm) Laser fluence: 1-200 J/cm ²
Co ₃ O ₄ NP	Co	H ₂ O [12]	Nd: YAG laser (355 nm) Laser energy: 30 mJ/pulse
Cubic-BN NP	Hexagonal-BN	Acetone [13]	Nd: YAG laser (532 nm) Power density: 10 ¹⁰ W/cm ²
Cubic-C ₃ N ₄ NR	Graphite	Ammonia [14]	Nd: YAG laser (532 nm) Power density: 10 ¹⁰ W/cm ²
Diamond NP	Graphite	Acetone [15] H ₂ O [16]	Nd: YAG laser (532 nm) Power density: 10 ¹⁰ W/cm ² Nd: YAG laser (532 nm) Laser energy: max 125 mJ/pulse
Hf ₂ S NP	HfS ₃	Tert-butyl disulfide [17]	Nd: YAG laser (532 nm) Laser energy: 30-50 mJ/pulse
Mg(OH) ₂ Tubular	Mg	H ₂ O +SDS [18]	Nd: YAG laser (355 nm) Laser energy: 100 mJ/pulse
Pt/TiO ₂ NP	Pt/TiO ₂	H ₂ O [19]	Nd: YAG laser (355 nm) Laser power: 160 mJ/pulse
SnO ₂ NP	Sn	H ₂ O +SDS [20]	Nd: YAG laser (355 nm) Laser energy: 100 mJ/pulse
TiO ₂ NP	Ti	H ₂ O H ₂ O +SDS [21, 22]	Nd: YAG laser (355 nm) Laser energy: max 150 mJ/pulse
ZnO NP core-shell	Zn	H ₂ O +SDS [23] H ₂ O [24]	Nd: YAG laser (1064 nm) Laser energy: 70 mJ/pulse
ZnO NP	Zn	H ₂ O +LDA H ₂ O +CTAB	Nd: YAG laser (355 nm) Laser energy: max 3.2 J/cm ²
Zn(OH) ₂ layer	Zn	H ₂ O +SDS [25]	Nd: YAG laser (355 nm) Laser energy: 100 mJ/pulse

These studies clearly indicate that LP-PLA has become a successful material fabrication technique, allowing versatile design through choosing suitable solid targets and confining liquids. Compared to the conventional physical methods (including chemical vapour deposition [26], vapour phase transport [27], and pulsed laser ablation in vacuum [28]), and chemical methods (including hydrothermal methods [29], soft-template [30] and use of various surfactants [31, 32]), the technique of LP-PLA has many distinct advantages. These include (i) a chemically ‘simple and clean’ synthesis, the final product is usually obtained without byproducts and no need for further purification; (ii) low cost of experimental setup and easily controlled parameters; (iii) the extreme confined conditions and induced high temperature, high pressure region favour the formation of unusual metastable phases. These advantages allow the designer to combine selected solid targets and liquid to fabricate compound nanostructures with desired functions.

§ 2.2 Fundamental aspects of LP-PLA

LP-PLA involves focusing a high power laser beam onto the surface of a solid target, which is submerged beneath a liquid. The interaction of the laser with the target causes the surface to vaporise in the form of an ablation plume, which contains species such as atoms, ions, and clusters, travelling with high kinetic energy. The species in the plume collide and react with molecules of the surrounding liquid, producing new compounds containing atoms from both the original target and the liquid. Due to the intensity of the laser and the nanosecond timescales, the instantaneous temperatures and pressures within the reaction volume can be extreme (many thousands of K at tens of GPa) [33]. Such high temperature, high pressure, and high density conditions provide a ‘brute force’ method of synthesising novel materials that have hitherto been inaccessible using milder, more conventional techniques.

The process of LP-PLA can be seen with reference to Figure 1. A typical setup has a short-pulsed high power laser source *e.g.* Nd:YAG, Cu vapour, or Ti:sapphire, focused using a lens to a small spot onto a target. The solid target is placed in a holder and submerged under variable levels (several millimetres) of

liquid. The liquid-containing vessel may be open, or have a window flush with the liquid in order to prevent splashing. Laser pulses are then fired at the target for a duration of time (minutes to hours) in order to cause ablation.

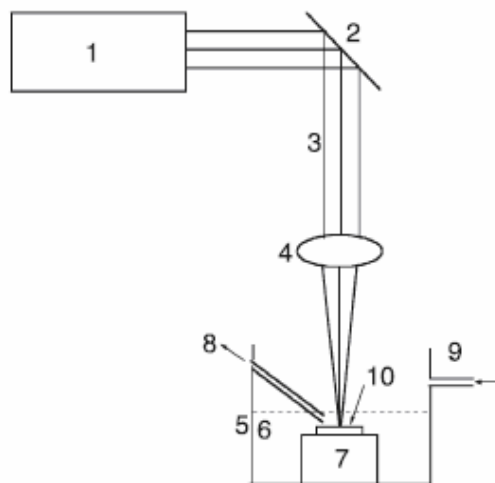


Figure 2.1 Schematic diagram of a typical LP-PLA setup: (1) laser *e.g.* Nd-YAG; (2) reflecting mirror; (3) laser beam; (4) focusing lens; (5) chamber; (6) liquid; (7) target holder; (8) collecting pipe (optional); (9) effusion pipe (optional); (10) target (reproduced from [34]).

The initial process of laser ablation is the interaction of light with the solid target surface which causes vaporisation of the solid target and a small amount of surrounding liquid. Chemical reactions between the ablated species and molecules in the liquid can subsequently occur as the ejected species are highly excited, both electronically and translationally [35]. The reaction products are typically NPs composed of atoms from both the target and the liquid, which form a suspension in the liquid. Due to the accumulation of these NPs in the surrounding liquid (forming a colloidal solution), prolonged interaction with the laser radiation may occur, leading to further changes in the NP's composition, size or morphology [36].

Formation of NPs using laser ablation of solids, either in gas or in vacuum, has been extensively explored during the last decade. By using different target materials and background gases, and varying parameters such as the laser wavelength, fluence, and pulse duration, it is possible to produce a wide variety of

compounds [37]. LP-PLA can be seen as the extension of this concept. Therefore, the process of laser interaction with the target is similar for both laser ablation in a vacuum and ablation at the solid-liquid interface. Both produce plasmas and create a strong confinement of the emission species, resulting in an efficient electron-ion recombination. The difference occurs when the plasma begins to expand, which occurs freely in vacuum, but is confined by any liquid layer. The liquid delays the expansion of the plasma, leading to a high plasma pressure and temperature, which allows the formation of novel materials. Another advantage is that both the solid target and the liquid are vaporised, so the product can contain atoms from the target material and the liquid. The generation of various NPs by LP-PLA is an alternative to the well-known chemical vapour deposition (CVD) method, and is characterized by its relative simplicity and the low cost of the experimental setup. Moreover, NPs produced by laser ablation of solid targets in a liquid environment are free of any counter-ions or surface-active substances [15].

§ 2.3 Materials produced by LP-PLA

§ 2.3.1 Nanometre-sized particles

LP-PLA has been used to produce NPs of many different metal elements including titanium [9,36], silicon [9], cobalt [12,38], zinc [39], copper [40], silver [9,36,41] and gold [9,36,41,42]. For example, in Fig 2.2(a), the Ag particles are flat disks and their thickness is of the order of a few nanometres [36]. This is clearly seen in those areas where the TEM image of intersection of two or more Ag particles appears darker than each separate particle (Figure 2.2(b)). This technique can also be used to prepare NPs of compound materials such as TiO₂ [43], CeO₂ [34], TiC [9] and CoO [44] in water, and ZnSe and CdS in various solvents, including water [45]. Furthermore, the method has also been used to convert structures such as hexagonal boron nitride crystals to cubic boron nitride crystals [46].

Due to the unique extreme high temperature and pressure conditions, LP-LPA has even been used to produce nanocrystalline diamond [15,47,48,49]. The carbon

phase diagram (Figure 2.3) shows region C, wherein LP-LPA converts graphite to diamond. Furthermore, Yang and Wang have shown that this transformation occurs efficiently with probability 10^{-3} - 10^{-4} , an order of magnitude higher than in region A and via an intermediate rhombohedral phase [48]. They produced nanocrystalline diamonds by LP-PLA (using a Nd:YAG laser, with a pulse width of 10 ns) of a graphite target under 1-2 mm of water [50]. Figure 2.4(a) shows a TEM image of the nanocrystalline diamonds at the nanometre scale. Indexing the Selected Area Electron Diffraction (SAED) pattern (Figure 2.4(b)), confirmed the conversion of graphite to diamond. It is very interesting that a mixture of a cubic and hexagonal diamond phase was observed in their experiment.

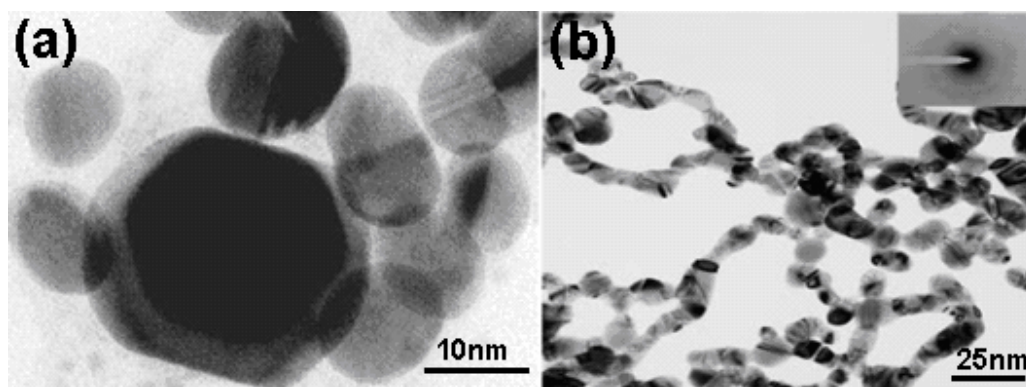


Figure 2.2 (a) HRTEM view of Ag NPs obtained by ablation of bulk Ag in water. (b) TEM view of linked Au NPs produced at elevated laser fluence (35 J/cm^2) (reproduced from [36]).

In nanocrystalline diamond production it was originally thought that OH^- ions were needed from the liquid phase to etch non-diamond species from the surface, thereby allowing diamond to form preferentially. However, subsequent experiments [47], using cyclohexane as the liquid, also produced nanocrystalline diamond, and thereby proved that the mechanism does not need OH^- and is likely to be purely physical in nature.

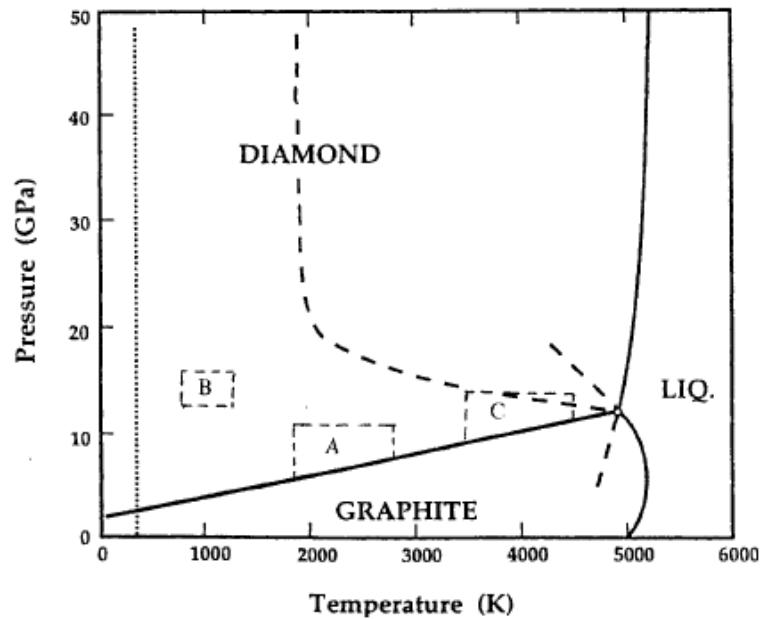


Figure 2.3 The carbon phase diagram. Regions obtainable via: (A) shock wave; (B) high temperature high pressure compression, and (C) LP-LPA production methods (reproduced from [48])

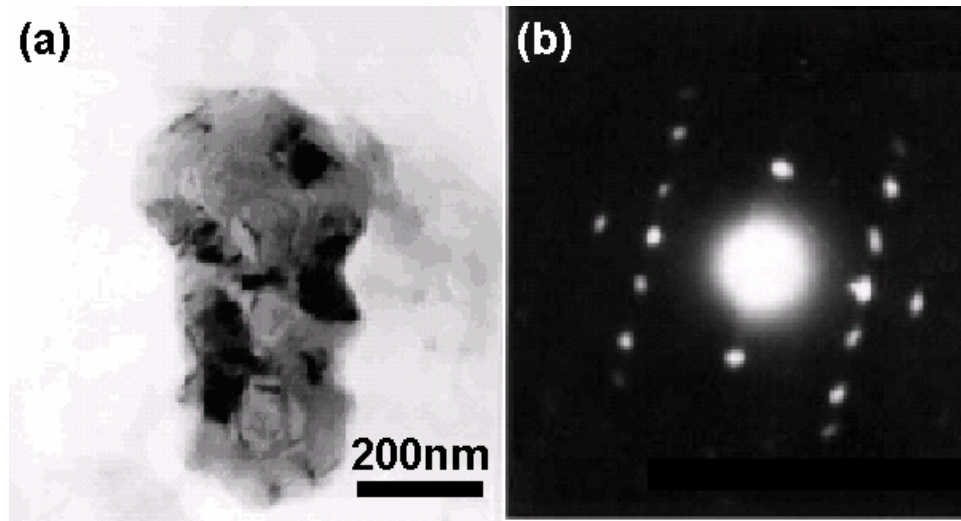


Figure 2.4 (a) The morphology and (b) the corresponding SAED pattern of LP-PLA-prepared diamond crystals. A single diamond grain has an intergrowth crystal which has both hexagonal and cubic structure (reproduced from [50])

For diamond production by LP-PLA to date, the choice of the liquid phase has had no effect on the species formed. However liquids can be selected that will react with the ablated target material. Carbon nitride nanocrystals have been produced by ablating a solid graphite target in ammonia solution [51], titanium carbide has been made using a titanium target and dichloroethane, and silicon dioxide is formed by silicon ablation in water [36].

§ 2.3.2 One-dimensional nanostructures

One-dimensional structures, such as needles or nanorods (NRs), can also be made by LP-PLA. For example, NRs of immiscible silver-nickel alloy have been synthesized by this method [52]. The typical diameters of these NRs were in the range of 30-50 nm, and the lengths were in the range of 300-500 nm, as shown in Figure 2.5. From the inset of Figure 2.5(b), the composition of the NR was found to be silver and nickel, confirmed by Energy Dispersive X-ray spectroscopy (EDX).

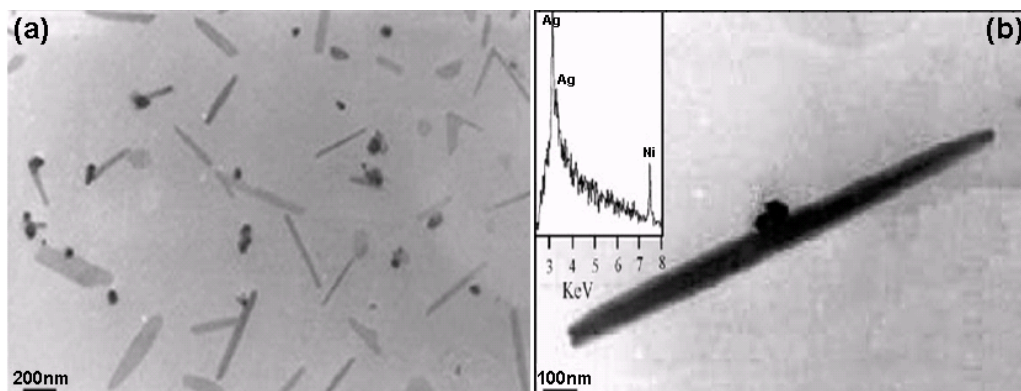


Figure 2.5 (a) TEM bright field image of immiscible silver-nickel alloy NRs synthesized by LP-PLA at the nickel-silver nitrate solution interface, (b) TEM bright field image of a single crystalline Ag-Ni alloy NR, EDX spectrum (inset) confirms that the NR is composed of Ag and Ni (reproduced from [52]).

It was reported by Wang *et. al* [53] that carbon nanotubes (CNTs) can also be produced by laser ablation of a graphite sample immersed in water (see Figure 2.6). The experiment revealed the dependence of CNT production on the structure of the target. The more perfect the layer structure of the graphite sample, the easier the production of the CNTs. Production of the CNTs was also affected by the orientation of the lattice at the surface of the graphite sample. Glassy carbon did not produce CNT. The water quenched the laser-vaporized species at the surface of the sample so as to provide the reactive material for the growth of the CNTs. The perfect crystal lattice of the graphite sample surface distributed the vaporized material nearly two-dimensionally, and the environment favoured the production of the CNTs.

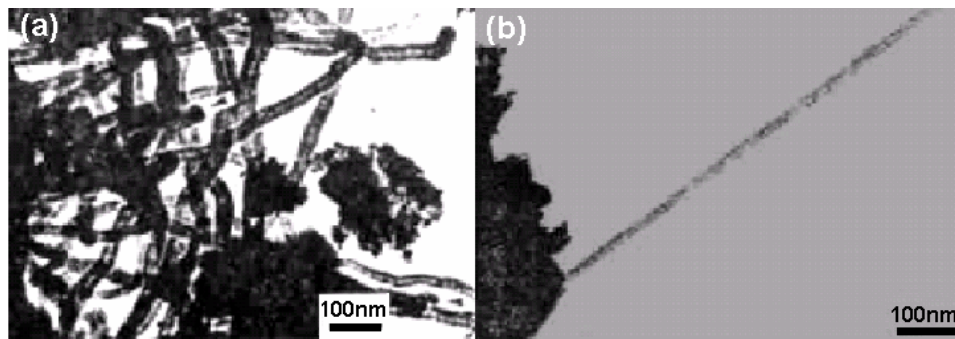


Figure 2.6 CNTs prepared at graphite-water interface by LP-PLA. (a) Network distributed CNT from highly oriented pyrolytic graphite (HOPG), (b) single CNT (reproduced from [53]).

§ 2.3.3 Higher-dimensional ordering

Only very recently has LP-PLA gained intensive attention for its ability to form more complex, higher dimensional nanostructures, and instigated the study of the dynamical process among laser-solid-liquid interactions. Liang and co-workers first reported the formation of an interesting layered zinc hydroxide/dodecyl sulfate (designated as ZnDS) structure and ZnO NPs, by laser ablation of Zn in SDS solution and pure water using the third harmonic of a Nd: YAG laser at a wavelength of

355 nm [54,55]. Adopting a similar method, Zeng and co-workers successfully prepared Zn/ZnO core/shell NPs by changing the laser wavelength to 1064 nm [56]. In Figure 2.7(a) NPs obtained from 0.05 M SDS solution with 70 mJ/pulsed have a nearly spherical shape and average size about 20 nm. HRTEM examination has revealed that the NPs actually have a core-shell structure, and the shell thickness reduced from about 8 to 2.5 nm with decrease of laser power from 100 to 35 mJ/pulse. Figure 2.7(b) and (c) show the typical core-shell NPs with shell thicknesses of 6 and 2.5 nm, respectively, corresponding to laser powers of 70 and 35 mJ/pulse. Further analysis of the lattice fringes has demonstrated that the Zn core and ZnO shell are composed of many ultrafine nanocrystals with different lattice orientations (see circular areas marked in Figure 2.7(d)) and of a great deal of disordered areas at the boundaries between these nanocrystals, which are expected to influence its properties greatly.

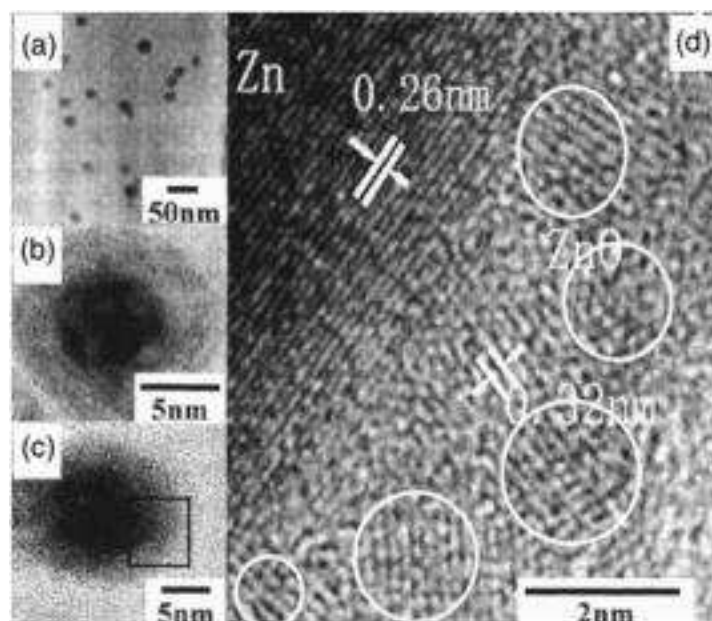


Figure 2.7 TEM images of the samples obtained from LP-PLA of 0.05 M SDS solution using different laser powers: (a) Sample obtained by laser ablation with 70 mJ/pulse, (b) HRTEM image of a typical particle in sample (a), (c) HRTEM image of a typical particle with 35 mJ/pulse, and (d) local magnified image

corresponding to the framed region marked in image (c). The circles in image (d) show the ultrafine nanocrystals in the shell (reproduced from [56]).

Further work by Zeng and co-workers [57] proved that these NPs can be self-assembled into treelike nanostructures after aging of the stable colloidal solution for enough time at room temperature without any further heating treatment. TEM observation has revealed that the NPs were isolated before aging (Figure 2.8(a)), but after aging, most of these separated particles assembled into treelike nanostructures, as shown in Figure 2.8(b). The assembled products have a rough surface and a multibranched structure, and their sizes are much larger than those of the original NPs (the diameters of the branches are about 100 nm). The SAED patterns in Figure 2.8(c) and (d) correspond to the isolated NPs and the edge of the assembled treelike nanostructures. The NPs exhibit a typical ZnO nanocrystal pattern. However, the treelike nanostructures have two sets of diffraction spot patterns, corresponding to Zn and ZnO, indicating the Zn/ZnO dual components in the treelike assemblies. The pattern composed of nearest diffraction spots is not a regular hexagon, but has a vertex angle of 81° (instead of 60° as usually expected). The slight distortion of the diffraction pattern could be ascribed to the lattice distortion, to some extent caused by the laser-induced non-equilibrium process, including high temperature, high pressure, and ultrarapid reactive quenching.

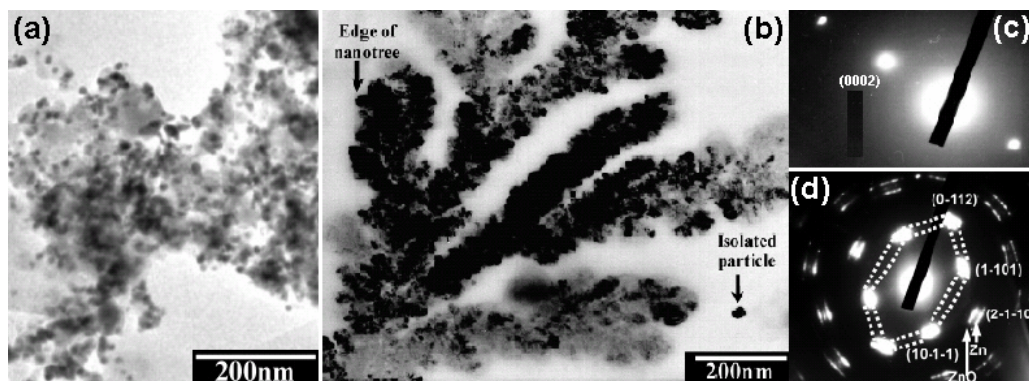


Figure 2.8 TEM images of the (a) as-prepared and (b) aged product from a stable 0.05 M SDS NP colloid. The SAED patterns for (c) the unassembled NPs and (d) the edge region of the self-assembled treelike nanostructures (reproduced from [57]).

Similar morphology was also observed in a silver oxide system. Liu *et al.* [58] reported that ablation at the solid-liquid interface of a nickel target in silver nitrate solution produced silver and silver oxide nanodendrites, as shown in Figure 2.9. All these works help to facilitate understanding of nanocrystal self-assembly behaviour, especially in the very ‘soft’ environment, and suggests that LP-PLA might be a promising method to fabricate highly ordered nanostructures based on a NP self-assembly process.

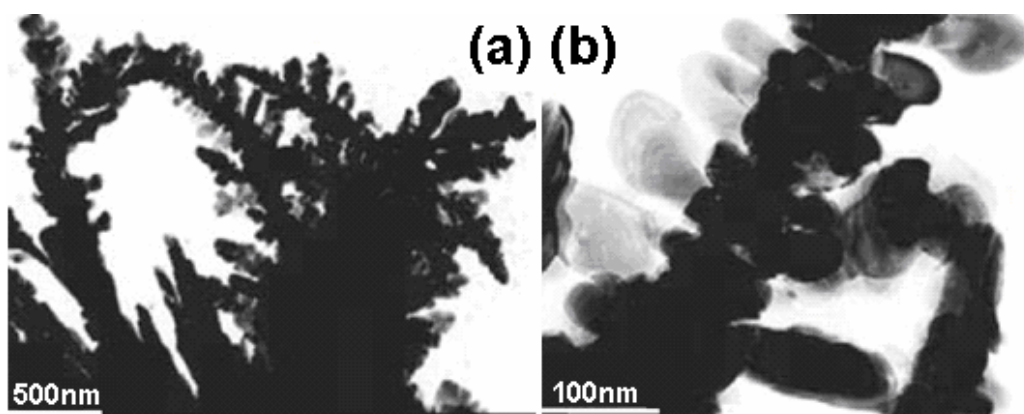


Figure 2.9 TEM bright field image of (a) fractal-like nanodendrites grown during LP-PLA in a silver nitrate solution. (b) detailed structures of silver nanoparticles and silver oxide nanoplates (reproduced from [58]).

§ 2.4 Liquid phase ablation mechanism

The mechanisms involved in the nucleation and phase transition of nanocrystals upon LP-PLA are not well understood. A recent review by Yang [59] gives an understanding of some of the nucleation thermodynamics, the phase transition, and the growth kinetics of nanocrystals by laser ablation of liquids. Therefore, here we shall only give a relatively brief introduction.

Generally, it is proposed that LP-PLA is very fast and far-from-equilibrium process, so that all metastable and stable phases forming at the initial, intermediate

and final stages of the conversion could be reserved in the final products, especially, for any metastable intermediate phases [48]. In other words, the quenching times in LP-PLA are so short that the metastable phases which form during the intermediate stage of the conversion can be frozen in, and form the synthesized final products.

According to Fabbro and co-workers [60], at the very initial stage of interaction of the high energy laser with the interface between the solid and the liquid, species ejected from the solid target surface have a large initial kinetic energy. Due to the covering effect of the liquid, these ejected species form a dense region in the vicinity of the solid-liquid interface. This stage is similar to that which occurs in vacuum or low pressure gas, where the laser generates a plasma ‘plume’. In LP-PLA, since the plasma is confined in the liquid, it expands adiabatically at supersonic velocity creating a shock-wave in front of it. This shock-wave will induce an extra, instantaneous pressure as it passes through the liquid. This ‘laser-induced pressure’ will result in the temperature increasing in the plasma [61,62]. Therefore, compared with a PLA plasma formed in gas or vacuum, the plasma formed in LP-PLA is higher pressure and higher density. Another effect of the localised high temperature is that a small amount of the surrounding liquid is vaporised to form bubbles within the liquid. As more material is vaporised, the bubbles expand, until, at a certain critical combination of temperature and pressure, they collapse [63]. It is believed that when the bubbles collapse, the nearby species are subjected to temperatures of thousands of K and pressures of several GPa, and that these extreme conditions allow novel materials to be created [33].

These ‘cavitation’ bubbles have been studied using a pressure transducer and photographic techniques [33,64], as well as a surface plasmon probe [63]. Shaw *et al.* [33] used a pressure transducer to measure the pressure variation at a solid-liquid interface induced by the formation and collapse of a cavitation bubble. The bubble was generated near the surface by a Nd:YAG laser operating at a wavelength of 1064 nm. Photographs of the bubble taken at various delay times after the laser pulse show the collapse of the bubble, shown in Figure 2.10. From (c) in Figure 2.10, the bubble surface furthest from the solid begins to flatten, showing the formation of a liquid jet, and by (d) the liquid jet threads the bubble and impacts upon the solid surface. The pressure begins to rise at this point, and continues to rise as more liquid

flows through the cavity. However, the sharp rise in pressure is attributed to shock-wave emissions, and not to the liquid jet. Figure 2.10(g) shows the shockwaves produced when the bubble reaches its minimum volume. The parts of the cavity closest to the solid boundary have undergone a noticeable elongation along the boundary wall, such that the top and bottom parts of the image of the bubble nearest the boundary are distorted away from the spherical shape. The bubble surface on the opposite side, furthest from the boundary, is relatively spherical. At maximum volume, the bubble appears to be attached to the solid boundary, *i.e.* there is no observable liquid layer between the two. The white dot visible inside the bubble positioned near the boundary is the laser-generated self-illuminating plasma which is caused by the laser breakdown process and marks the initial geometrical centre of the cavity.

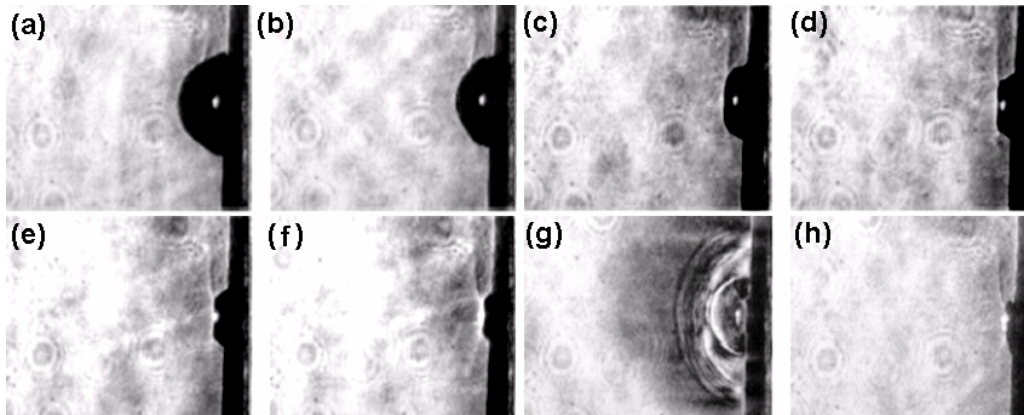


Figure 2.10 Schlieren images of an oscillating cavitation bubble in front of a solid boundary at times $t \approx$ (a) 110, (b) 170, (c) 200, (d) 210, (e) 215, (f) 217, (g) 220.5, (h) 224.5 μs . The horizontal bar in image (a) (bottom right corner) measures 1 mm (reproduced from [33]).

§ 2.5 Conclusions

In recent years, laser ablation of a solid target in a confining liquid has been demonstrated to be an effective and general route to synthesize a various range of

nanocrystals and nanostructures. One of the main advantages of LP-PLA is that in contrast to other methods, it produces nanoparticles free of any counter-ions or surface active substances. LP-PLA is a one-step, direct and very simple preparation procedure, requiring room temperature and pressure only, and therefore may be more suitable for certain commercial applications. Furthermore, as ablation takes place at the solid-liquid interface, vaporisation of the liquid phase can also take place allowing it to be easily incorporated into the formation of final structures and locally confined modification of materials. In LP-PLA the excited ablated species are also able to undergo chemical reactions with the liquid phase leading to new materials. The produced NPs are free to transport themselves to any substrate or device systems, which can functionalize the desired properties.

The dominant mechanism of LP-PLA induces much higher temperatures and pressures than other PLA techniques, and hence it can form novel materials *e.g.* with metastable phases. Unlike PLA in gas or vacuum, the nucleation and growth of nanocrystals, are rapidly quenched in the liquid phase, leading to non-equilibrium conditions. This short quenching time can also result in the growth of small, nanometre-diameter crystals *e.g.* nanocrystalline diamond.

Much progress has been made recently to use LP-PLA to fabricate more complex structures, such as ZnO core-shell, treelike nanostructures, and silver oxide nanodendrites. To date, most nanomaterials reported by LP-PLA have been either continuous film structures, zero-dimensional (0D) NPs, or one-dimensional (1D) NRs. Since the 0D and 1D nanocrystals can serve as building blocks in forming two-dimensional or three-dimensional complex architectures with long term periodic structures (see chapter 1 for details), it should be expected that the LP-PLA approach would have great potential as a means to grow large arrays of hierarchical, complex, oriented and ordered superstructures. Therefore, the following chapters are mainly concerned with the development of the LP-PLA technique and its extension to fabricate not just nanoparticles and nanorods, but also higher dimensional ordered architectures. We aim to maximize the applications using this novel method, and to try to understand the underlying mechanisms involved in this complex process.

Bibliography

- [1] Dijkkamp D, Venkatesan T, Wu X D, Shaheen S A, Jisrawi N, Minlee Y H, Mclean W L, Croft M, *Appl. Phys. Lett.*, 1987, **51**, 619.
- [2] Radhakrishnan G, Adams P M, *Appl. Phys. A*, 1999, **69**, S33.
- [3] Pappas D L, Saenger K L, Bruley J, Krakow W, Cuomo J J, Gu T, Collins R W, *J. Appl. Phys.*, 1992, **71**, 5675.
- [4] Loir A S, Garrelie F, Donnet C, Belin M, Forest B, Rogemond F, Laporte P, *Thin Solid Films*, 2004, **453**, 531.
- [5] Patil P P, Phase D M, Kulkarni S A, Ghaisas S V, Kulkarni S K, Kanetkar S M, Ogale S B, Bhide V G, *Phys. Rev. Lett.*, 1987, **58**, 238.
- [6] Ogale S B, *Thin Solid Films*, 1988, **163**, 215.
- [7] Pyatenko A, Shimokawa K, Yamaguchi M, Nishimura O, Suzuki M, *Appl. Phys. A.*, 2004, **79**, 803.
- [8] Tsuji T, Iryo K, Watanabe N, Tsuji M, *Appl. Surf. Sci.*, 2002, **202**, 80.
- [9] Dolgaev S I, Simakin A V, Voronov V V, Shafeev G A, Bozon-Verduraz F, *Appl. Surf. Sci.*, 2002, **186**, 546.
- [10] Tarasenko N V, Butsen A V, Nevar E A, Savastenko N A, *Appl. Surf. Sci.*, 2006, **252**, 4439.
- [11] Compagnini G, Scalisi A A, Puglisi O, *J. Appl. Phys.*, 2003, **94**, 7874.
- [12] Tsuji T, Hamagami T, Kawamura T, Yamaki J, Tsuji M, *Appl. Surf. Sci.*, 2005, **243**, 214.
- [13] Wang J B, Yang G W, Zhang C Y, Zhong X L, Ren ZH A, *Chem. Phys. Lett.*, 2003, **367**, 10.
- [14] Yang G W, Wang J B, *Appl. Phys. A*, 2000, **71**, 343.
- [15] Wang J B, Zhang C Y, Zhong X L, Yang G W, *Chem. Phys. Lett.*, 2002, **361**, 86.
- [16] Yang L, May P W, Yin L, Smith J A, Rosser K N, *Diamond Relat. Mater.*, 2007, **16**, 725.

- [17] Nath M, Rao C N R, Popvitz-biro R, Albu-Yaron A, Tenne R, *Chem. Mater.*, 2004, **16**, 2238.
- [18] Liang C H, Sasaki T, Shimizu Y, Koshizaki N, *Chem. Phys. Lett.*, 2004, **389**, 58.
- [19] Sasaki T, Liang C H, Nichols W T, Shimizu Y, Koshizaki N, *Appl. Phys. A*, 2004, **79**, 1489.
- [20] Liang C H, Shimizu Y, Sasaki T, Koshizaki N, *J. Phys. Chem. B*, 2003, **107**, 9220.
- [21] Liang C H, Shimizu Y, Sasaki T, Koshizaki N, *Appl. Phys. A*, 2005, **80**, 819.
- [22] Liang C H, Shimizu Y, Sasaki T, Koshizaki N, *J. Mater. Res.*, 2004, **19**, 1551.
- [23] Zeng H B, Cai W P, Hu J L, Duan G T, Liu P S, Li Y, *Appl. Phys. Lett.*, 2006, **88**, 171910.
- [24] Ishikawa Y, Shimizu Y, Sasaki T, Koshizaki N, *J. Colloid Interf. Sci.*, 2006, **300**, 612.
- [25] Usui H, Sasaki T, Koshizaki N, *Appl. Phys. Lett.*, 2005, **87**, 063105.
- [26] Kempa K, Kimball B, Rybczynski J, Huang Z P, Wu P F, Steeves D, Sennett M, Giersig M, Rao D V G L N, Carnahan D L, Wang D Z, Lao J Y, Li W Z, Ren Z F, *Nano Lett.*, 2003, **3**, 13.
- [27] Duan X F, Lieber C M, *Adv. Mater.*, 2000, **12**, 298.
- [28] Sun Y, Fuge G M, Fox N A, Riley D J, Ashfold M N R, *Adv. Mater.*, 2005, **17**, 2477.
- [29] Yang H G, Zeng H C, *J. Phys. Chem. B*, 2004, **108**, 3492.
- [30] Mirkin C A, Letsinger R L, Mucic R C, Storhoff J J, *Nature*, 1996, **382**, 607.
- [31] Sun Y G, Gates B, Mayers B, Xia Y N, *Nano Lett.*, 2002, **2**, 165.
- [32] Li Y D, Li X L, Deng Z X, Zhou B C, Fan S S, Wang J W, Sun X M, *Angew. Chem. Int. Ed.*, 2002, **41**, 333.
- [33] Shaw S J, Schiffers W P, Gentry T P, Emmony D C, *J. Phys. D*, 1999, **32**, 1612.
- [34] Chen J W, Dong Q Z, Yang J, Guo Z X, Song Z L, Lian J S, *Mater. Lett.*, 2004, **58**, 337.
- [35] Sakka T, Iwanaga S, Ogata Y H, Matsunawa A, Takemoto T, *J. Chem. Phys.*, 2000, **112**, 8645.

- [36] Simakin A V, Voronov V V, Kirichenko N A, Shafeev G A, *Appl. Phys. A*, 2004, **79**, 1127.
- [37] Henley S J, Ashfold M N R, Cherns D, *Surf. Coat. Tech.*, 2004, **177**, 271.
- [38] Dolgaev S I, Simakin A V, Voronov V V, Shafeev G A, Bozon-Verduraz F, *Appl. Surf. Sci.*, 2002, **186**, 546.
- [39] Zeng H B, Cai W P, Li Y, Hu J L, Liu P S, *J. Phys. Chem. B*, 2004, **109**, 18260.
- [40] Yeh M S, Yang Y S, Lee Y P, Lee H F, Yeh Y H, Yeh C S, *J. Phys. Chem. B*, 1999, **103**, 6851.
- [41] Shafeev G A, Freysz E, Bozon-Verduraz F, *Appl. Phys. A*, 2004, **78**, 307.
- [42] Sylvestre J P, Poulin S, Kabashin A V, Sacher E, Meunier M, Luong J H T, *J. Phys. Chem. B*, 2004, **108**, 16864.
- [43] Sugiyama M, Okazaki H, Koda S, *Jpn J. Appl. Phys.*, 2002, **41**, 4666.
- [44] Tsuji T, Hamagami T, Kawamura T, Yamaki J, Tsuji M, *Appl. Surf. Sci.*, 2005, **243**, 214.
- [45] Ankin K V, Melnik N N, Simakin A V, Shafeev G A, Voronov V V, Vitukhonovsky A G, *Chem. Phys. Lett.*, 2002, **366**, 357.
- [46] Wang J B, Yang G W, Zhang C Y, Zhong X L, Ren Z A, *Chem. Phys. Lett.*, 2003, **367**, 10.
- [47] Pearce S R J, Henley S J, Claeysens F, May P W, Hallam K R, Smith J A, Rosser K N, *Diam. Rel. Mater.*, 2004, **13**, 661.
- [48] Yang G W, Wang J B, *Appl. Phys. A*, 2001, **72**, 475.
- [49] Wang J B, Yang G W, *J Phys.:Condens. Mater.*, 1999, **11**, 7089.
- [50] Yang G W, Wang J B, Liu Q X, *J. Phys.: Condens. Matter*, 1998, **10**, 7923.
- [51] Yang G W, Wang J B, *Appl. Phys. A*, 2000, **71**, 343.
- [52] Liu Q X, Wang C X, Zhang W, Yang G W, *Chem. Phys. Lett.*, 2003, **382**, 1.
- [53] Wang Y H, Zhang Q, Liu Z Y, Huang R B, Zheng L S, *Acta physico-chimica Sinica*, 1996, **10**, 905.
- [54] Liang C H, Shimizu Y, Masuda M, Sasaki T, Koshizaki N, *Chem. Mater.*, 2004, **16**, 963.
- [55] Usui H, Sasaki T, Koshizaki N, *Chem. Lett.*, 2005, **34**, 700.

- [56] Zeng H B, Cai W P, Cao B Q, Hu J L, Li Y, Liu P S, *Appl. Phys. Lett.*, 2006, **88**, 181905.
- [57] Zeng H B, Liu P S, Cai W P, Cao X L, Yang S K, *Cryst. Growth Des.*, 2007, **7**, 1092.
- [58] Liu Q X, Wang C X, Yang G W, *Eur. Phys. J. B*, 2004, **41**, 479.
- [59] Yang G W, *J Prog. Mater. Sci.*, 2007, **52**, 648.
- [60] Barther L, Fabbro R, Peyre P, Tollier L, Bartinicki E, *J. Appl. Phys.*, 1997, **89**, 2836.
- [61] Zhu S, Lu Y F, Hong M H, Chen X Y, *J. Appl. Phys.*, 2001, **89**, 2400.
- [62] Zhu S, Lu Y F, Hong M H, *Appl. Phys. Lett.*, 2001, **79**, 1396.
- [63] Yavas O, Schilling A, Bischof J, Boneberg J, Leiderer P, *Appl. Phys. A*, 1997, **64**, 331.
- [64] Tsuji T, Tsuboi Y, Kitamura N, Tsuji M, *Appl. Surf. Sci.*, 2004, **229**, 365.